Beyond Arrows: Natural Ventilation in a High-Rise Building with Double Skin Façade

MONA AZARBAYJANI
University of North Carolina at Charlotte

INTRODUCTION

Naturally Ventilated Double Skin Facades

The concept of DSF is not new and dates back to many years ago where in central Europe; many houses utilized box-type windows to increase thermal insulation (Oesterle, 2000). The double-skin façade is an architectural phenomenon driven by the aesthetic desire for an all-glass façade and the practical desire to have natural ventilation for improved indoor air quality in buildings. Until recently the use of double-skin facades had became more popular in many high-rise buildings in Europe.

A number of studies, research and several simulation programs have been done on employing the natural ventilation in buildings and thermal performance of double skin facades. Most of them have been carried out for solar chimneys -one way to increment natural ventilation and to improve indoor air quality- and Trombe walls prior to double skin facades. Most of them found out the natural ventilation is possible in summer even for multistory buildings (Wong, 2006). The potential of using a double façade for natural ventilation of the building in climates other than europe has not been fully studied though. A number of interesting investigations and findings are reported in the literature pertaining to passive ventilation in buildings with double-skin facades.

It was found that significant energy savings are possible if natural ventilation could be exploited through the use of a double-skin facade (DSF). For example, the Loyola University Information Commons and Digital Library in Chicago integrated natural ventilation with a DSF to cool the buildings. The results indicated that an integrated facade can reduce 30 percent of energy consumption (52 days operated in natural mode) (Frisch, 2005).

Even though most of the research has been done in temperate climate conditions, studies have revealed a close link between natural ventilation design and the DSF function. Grabe et al. (2002) developed a simulation algorithm to investigate the temperature behavior and flow characteristics of natural-convection DSFs through solar radiation. It was found that the air temperature increased near heat sources that are close to window panes and shading device. Gratia and Herde (2007a, 2007b, 2007c) attempted to look at natural ventilation strategies, greenhouse effects, and the optimum position of sun- shading devices for DSFs facing south in a northern hemisphere temperate climatic. They found that a sufficient day or night ventilation rate can be reached by a window opening, even if wind characteristics are unfavourable.

METHODOLOGY

Natural ventilation is an essential part of sustainable building design. Energy conscious designers harness the cooling capacity of natural wind to increase indoor thermal comfort and ultimately save energy for active-space conditioning. Wind can cause air movement and perception of cooling, wind can bring in air of a different temperature and humidity. By numerically solving a series of conservation equations related to mass, momentum, and energy, computational fluid dynamics (CFD) tools help designers predict detailed airflow for special design cases and plan a building with optimal natural ventilation.

To preserve thermal comfort and reduce cooling loads, natural cooling strategies can be incorporated into buildings. In this study, the behavior of natural ventilation in a new double skin facade (DSF) configuration will be studied. To that end, Fluent, computational fluid dynamics software, was used to study the office airflow path. Developing a CFD model is a lengthy process. First, EnergyPlus-DesignBuilder was used to solve some boundary conditions, such as solar thermal energy. The temperature profile and air velocity within the DSF's cavity and the internal office space were simulated by Fluent, and, as a result, the offices' thermal comfort was calculated and presented. In this study, wind driven ventilation improved with stack effect in the noble configuration of DSF will be tested to see if it can maintain adequate comfort during summer and spring time in Chicago. The first step would be study the ambience which will be used as a boundary conditions in computational fludid dynamics tool. Initial studies of the macroclimate were carried out through Ecotect, which allowed for the efficient visualization of the local climatic conditions.

Assumptions

Simulations were performed with climatic data of Chicago (Midway airport). Weather data were recorded by the World Meteorological Organization and includes 12 actual months. Natural ventilation is possible during the shoulder season in Chicago. For this study, the months of May, June, September, and October were chosen.

The first stage of the air flow modeling is to construct a simple model of the innovative enclosure system the combined shaft-corridor DSF in Gambit. The numerical model is three-dimensional and the model is based on a control volume method. The geometric model of the entire building is constructed using a matrix of numbers to represent the points at which surfaces meet.

In the next stage, the boundary conditions were solved, the grid size refined, and number of necessary iterations determined. The generated model solved for wind velocity along with buoyancy forces. The model used to solve the iteration was bousinesqe in order to consider the buoyancy forces and in order to include wind force, the pressure at the surface boundary was calculated. In order to define the external boundary condition, the airflow needed to be solved for the external wind. For this study, only wind direction which is perpendicular to the DSF has been considered.

Wind Effects on High Rise Building

In assessing the effects of wind on buildings, it is important to consider the characteristic nature of the wind. The wind is turbulent, and this means speed varies with height.

Vertical profiles of mean wind speed for boundary layers are approximated by taking the wind speed to be proportional to the height raised to some power – a power law variation (Davenport,1965) the simple expression which is used extensively has the form :

$$V_h = 0.35 V_{met} h^{0.25}$$

Where V_h is the local wind speed at height, h, and V_{met} is the meteorological wind speed. Based on this formula, wind has been calculated for specific times that the CFD analysis was performed.

The wind speed from the meteorological data corresponds to the wind speed at 10 m height in open country. Since the building is located in an urban environment, the appropriate wind profile was assumed to be (0.35 and 0.25 are the constants which depends on the train in the vicinity of the buildings).

WIND PRESSURES

The distribution of wind pressure around a building depends very closely upon the local variation in wind velocity which the building produces. In accordance with the elementary pressure-velocity relationship, the pressure distribution is represented by a dimensionless pressure coefficient C_p :

$P_w = C_p \frac{\rho U_r^2}{2}$ Where,

P_w = wind pressure, Pa

ρ = air density, $^{kg}/_{m^3}$

V_r = wind speed at specified height, $^{m}/_{s}$

This formula has been used to calculate the boundary condition for the inlet and outlet pressure in Fluent.

The Geometry of the Cfd Model

The new configuration take the advantages of the strategies include ventilation driven by different combinations of wind and external stack. The most distinguishing feature of this configuration is its cooling stack towering over the south side of the building. This configuration combined both two shaft and corridor type through the building's facade. The cooling stacks allow for further ventilation on hot, stagnant summer days so the building can always remain cool within reasonable comfort levels.

Figure 1 shows how air flows through the chimney and provide ventilation inside each office module. Air gap inlet draw in fresh air at a low level and direct the fresh air into the room. The air exhausted through the outlet at the high-level gap of inner pane. Multi-storey chimneys suck exhausted air via a bypass opening at the top of the inner level. The vertical height of the glass chimney creates stronger uplift forces due to increased stack effect.

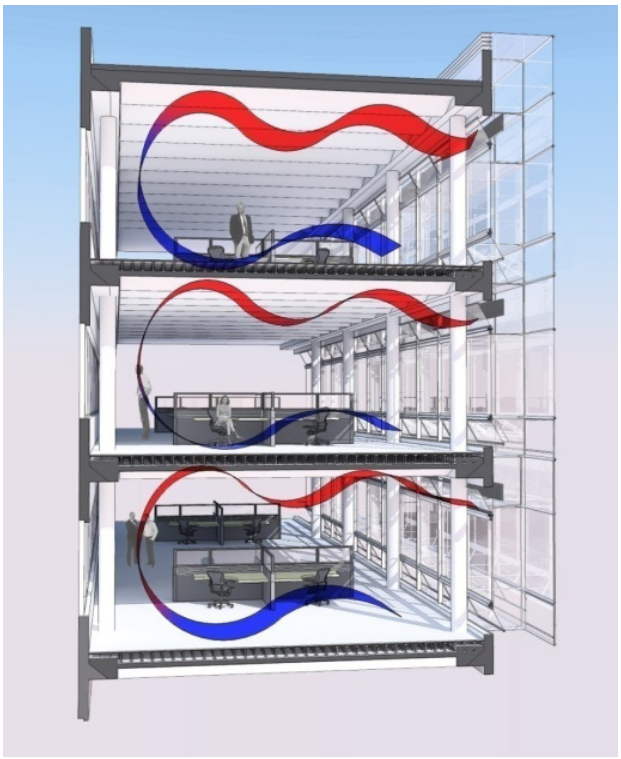

Figure 1. Intuitive diagrams Natural Ventilation and DSF (section of the new configuration)

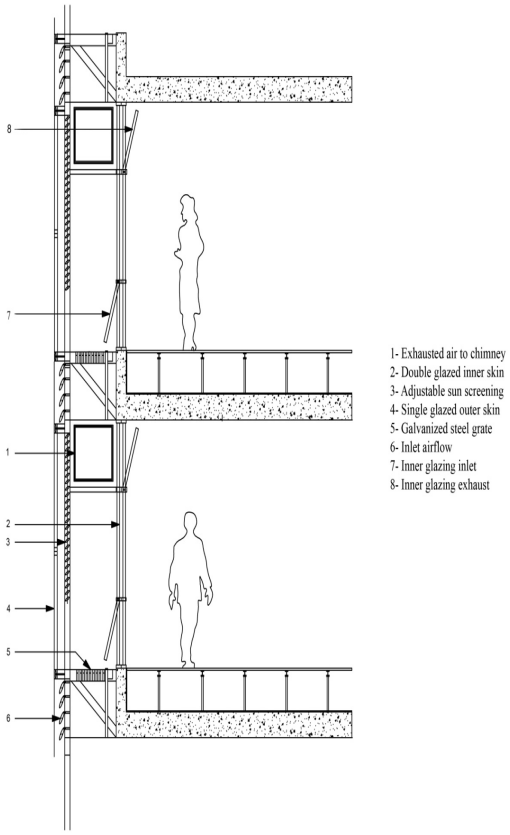

Figure 2. Vertical cross section of the new configuration of DSF

The effectiveness of ventilation driven by thermal buoyancy, or stack effect, is determined by the inlet air temperature, height between the inlet and outlet openings, size of these openings. Figure 2 shows the section of the modules and the configuration of openings inlet and exhasut.

MODEL DESCRIPTION

The first stage of CFD modeling is to construct a seven-story module with geometrical dimensions of 27x7 m, with 3.5 m ceiling height and 1.5 m cavity corridor in front of the offices in the Gambit. The simplified single skin facade of the model has openings on panes with 6mm thick glass. The DSF construction has one opening (inlet) at the outer pane and two openings (air inlet and exhaust) at the inner pane. The model is constructed in 3-D in Gambit as shown in the figures below.

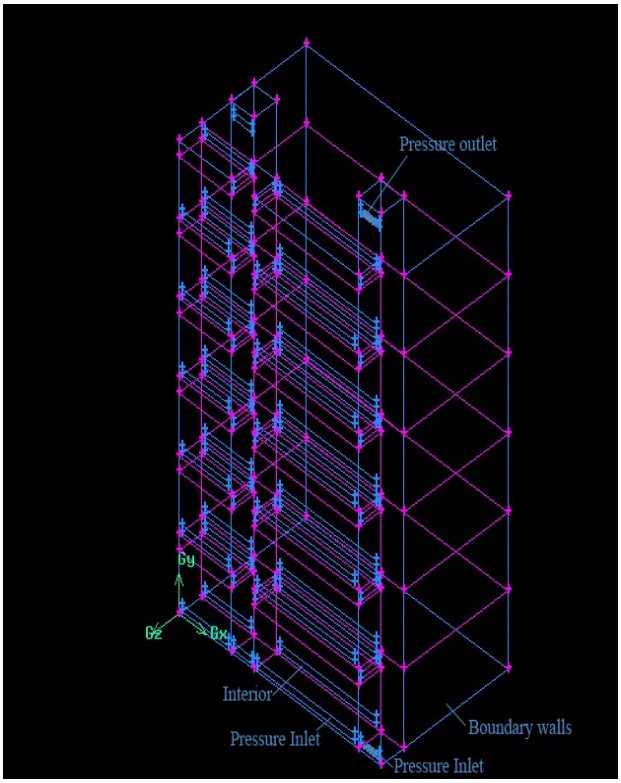

Figure 3. Model boundary settings

CFD MODEL BOUNDARY CONDITIONS

This study is going to model levels from the sixteenth to the twenty-third stories of a high-rise building. In the new configuration, the DSF has a ventilated shaft, which is 1.5x1.5 m with two openings on the lower and high chimney levels. This study introduces a shaft to improve the possibility of natural-ventilation stack effect to extract heat from the offices and improve airflow rates required to reach thermal comfort level within the interior.

The results of Fluent model of this seven story block looked at the velocity profile, airflow patterns, temperature within the double skin, and the internal office space. To calculate thermal comfort, the boundary conditions for wind velocity, external temperature and relative humidity were set to the ranges similar to Chicago climatic conditions and are presented in the Table 1.

SIMULATION RESULTS DEMONSTRATION

For the analysis of airflow and temperature in DSF and adjacent space, the combined shaft-corridor DSF has been generated and airflow patterns and temperature profile within the DSF has been illustrated for specific times of the year. Based on those data, the level of thermal comfort within the space will be predicted.

Cavity and Room Air Temperature

The location of the chimney openings in this shaft-corridor type in relation to the chimney exhaust will have an effect on the indoor thermal comfort and airflow velocity. It is a fact that the higher the exhaust opening is located from the inlet, the stronger stack effect within the air gap. This effect will then pull more air from office spaces to circulate throughout the building. The other factor that impacts on air velocity are inlet and outlet sizes. Due to the ventu-

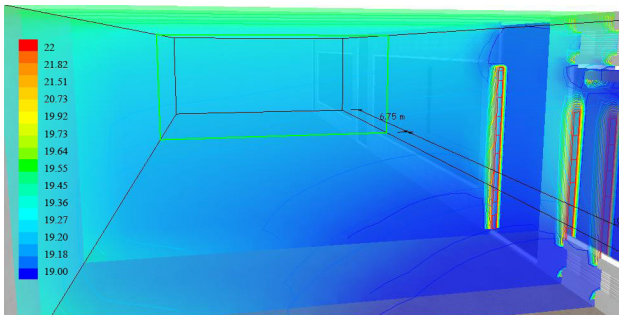

Figure 4. As displayed in fluent analysis of room temperature profile

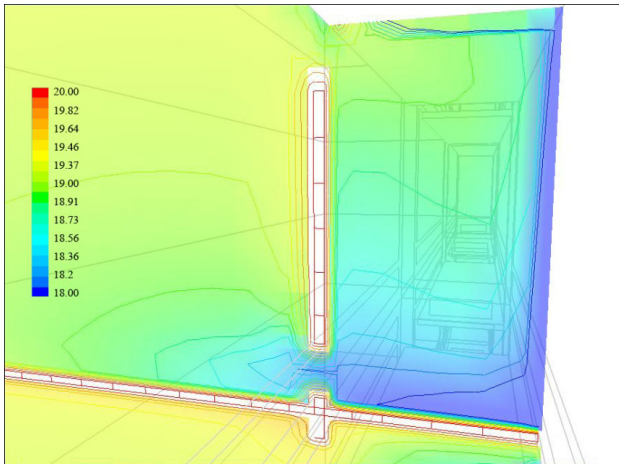

Figure 5. Cavity temperature gradient

Domain	
Domain material	Air at 20°C, 1 atm
Reference pressure	100,000 Pa (atmospheric pressure)
Reference temperature	295 K
Sources	
Buoyancy model	Boussinesq-calculates airflow from temperature difference rather than density difference.
Buoyancy reference temperature	Outdoor air temperature.
Gravitational acceleration	-9.81 m/s in the y-direction.
Boundary Conditions	
Side, top, bottom, & front domain boundary conditions	Openings with "deduced" air velocities, external temperature = outdoor air temperature at inflow only, external pressure at atmospheric pressure.
Back boundary conditions	Adiabatic solids (concrete) with depth = cavity Depth, glass: standard 6 mm clear glass.
Heat source (external glass)	11.43 W/m^2
Heat source (internal glass)	7.93 W/$m^2 m^{2^2}$
Walls heat	25 W/$m^2 m^2$
Velocity inlet	5 m/s
Cavity Details	
Cavity size	3.5 m high by 7 m wide by 1.5 deep.
Cavity external facade	Internal plate with surface temperatures on both sides is calculated based on heat source.
Cavity internal facade	External plate with surface temperature base on heat source.
Shaft and opening details	
Shaft size	1.5 m deep,1.5 long, 24.5 m high
DSF opening size for inner pane, air gap size (inlet and exhaust).	300 mm

Table 1. Model assumptions and inputs required by fluent

ry effect, the smaller the size, the more the velocity. Figure 4 illustrates the room's temperature gradient, which is clearly lower than the outside temperature of 20 °C. There is some temperature variation as the cavity is ventilated. The room air temperature increases towards the top as shown in Figure 4.

Figure 5 clearly illustrates an increase in the gradient temperature from the inlet to the outlet where higher-surface temperatures were reached due to accumulated heat and buoyancy effect.

As illustrated in previous figures, the interior air temperature is slightly higher than the exterior in the half of the room closer to the cavity and also in the half upper part. The temperature goes from 19 °C at the bottom opening to about 19.9 °C at the top opening. Figure 6 illustrates how the

temperature stratification ranges from low on the floor to highest close to the ceiling.

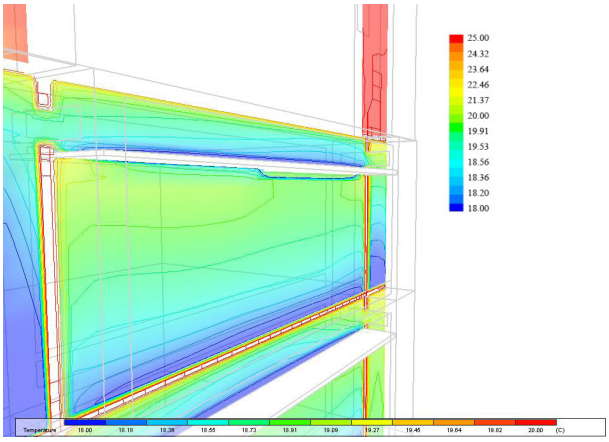

Figure 6. Cavity temperature profile-output from fluent

Figure 6 shows the cavity air temperature near the interior glazing. The temperature goes from 18 °C at the bottom opening to about 19.5 °C at the top opening. The stack air temperature increases towards the top of the chimney in a fairly linear progression, as shown qualitatively in Figure 7. All these figures depict the cavity model with 20° C outdoor air temperature and 480 watts/m2 incident solar energy obtained from the weather data. The interior air temperature is slightly higher than the lower half of the chimney air in average 1°C per floor.

A temperature contour study has shown that the office space's lower floors have lower internal temperatures compared to the higher floors. As we increase the shaft height, the upper floors would be hottest and probably uncomfortable for occupants during the summer month. It is interesting to discover that the office's mid-portion for all the floors are having higher temperatures compare to the front part. This could be due to the airflow pattern shown in the next section.

Airflow

The air velocity through the cavity is due to buoyancy and wind forces, and it is quite high. Figure 8 shows the building's air velocity model. The velocity in this model ranges from 7 m/s inlet to 2.3 m/s outlet of the chimney. The inflow from the external screen is 1 m/s and the internal

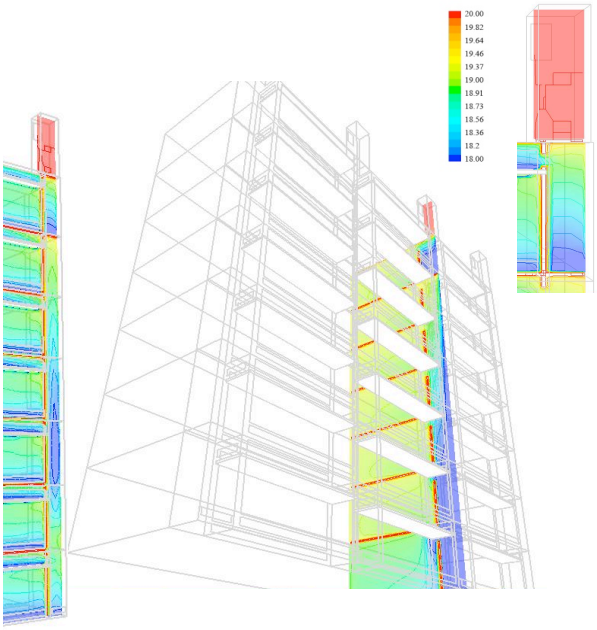

Figure 7. Chimney air temperature profile

screen inflow velocity is 0.45 m/s, while the exhaust airflow is 0.46 m/s on average. The exhaust air velocity to the chimney averages 1.3 m/s. The greatest velocity is near the inlet to the chimney and exhaust from the stack. As shown in the figure below, the velocities are increased relative to the one-story high cavity.

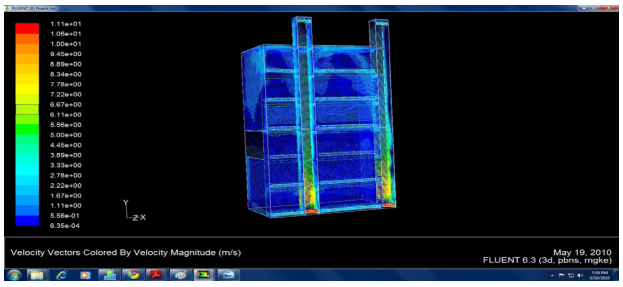

Figure 8. Model of air velocity vector in the building

Figure 9 shows the section of airflow at the opening of one story horizontally. Velocities are greatest near the opening, when the air is forced through the smaller area. In the back of the room, air velocities are high as they move toward the exhaust to get out from the stack. As illustrated in the figure below, air velocity in the chimney is higher close to the back wall of the chimney, and it is generally laminar when driven only by buoyancy without wind effects.

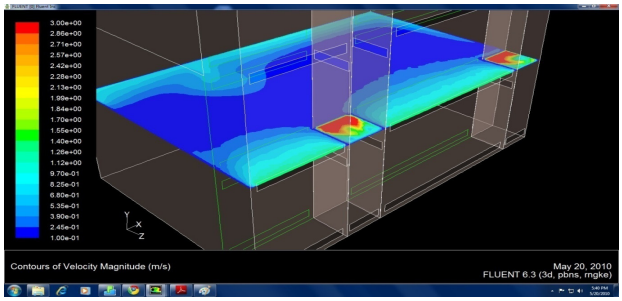

Figure 9. Horizontal velocity profiles

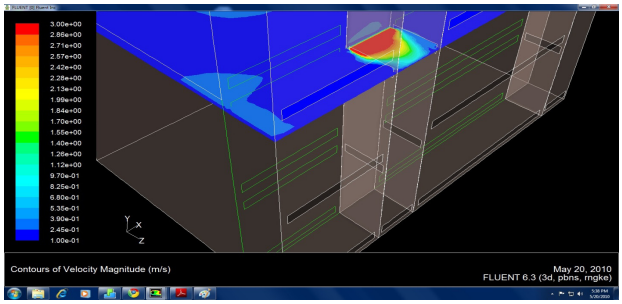

Figure 10. Horizontal velocity gradient

Figure 10 shows the horizontal velocity profile in the cavity and chimney. The velocity ranges from 0.46 m/s away from the surface and 0.97m/s near the opening. The greatest velocities are near the cavity openings where the wind impacts the airflow rate. Figure 15 shows velocity vectors at the openings of the chimney cavity model as analyzed in Figure 1 Velocities are greatest near the openings, when air is forced through the smaller area. In this model, the maximum velocity at the inlet is about 11 m/s. Other than at the openings, airflow through the chimney well is around 5 m/s and is driven by both wind and stack effect.

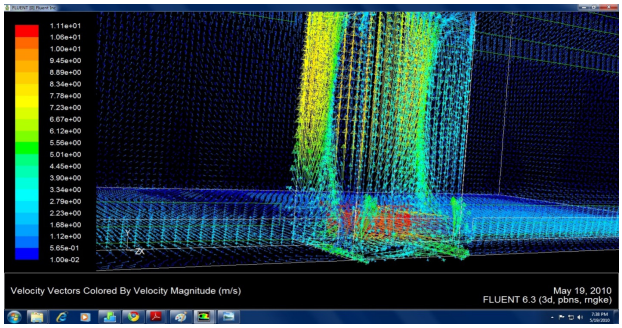

Figure 11. Model of air velocity close to the inlet opening

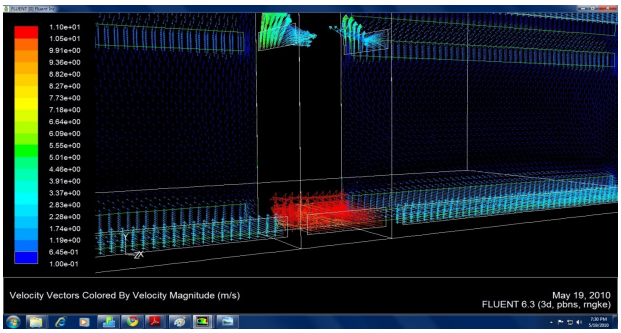

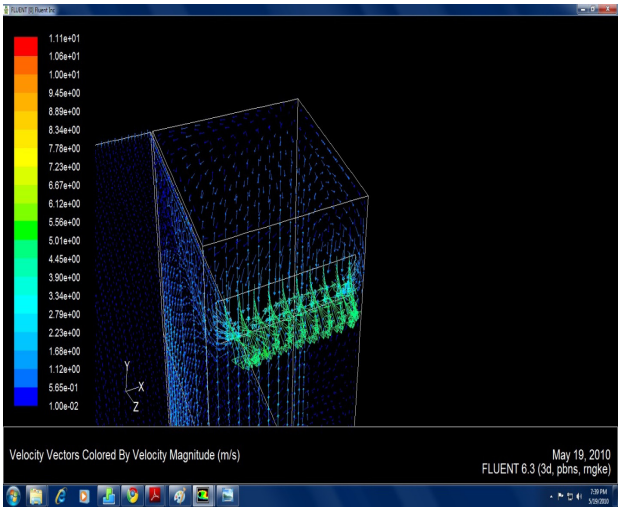

Figure 12. Airflow patterns and velocity at the chimney's outlet opening

A small turbulent flow forms at the stack inlet and outlet, and stack airflow is generally laminar when it is only driven by buoyancy.

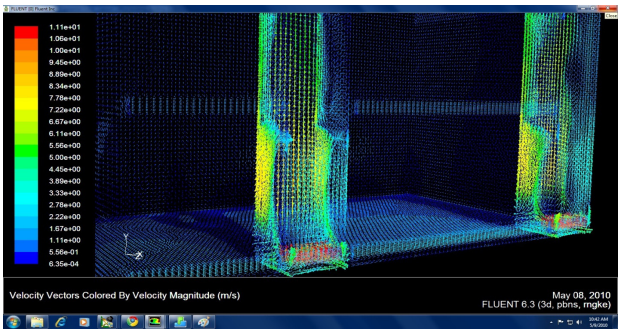

Figure 13. Air velocity vectors in the cavity and chimney

Figure 13 shows a vertical profile of air velocity vectors to the stack from the cavity. The velocity is quite high and it extracts hot stuffy air from offices

to the stack and outdoors. The airflow is likely to be more effective in extracting heat when the wind velocity is high and the temperature gradient occurs in the shaft increase the buoyancy effect.

Figure 13 shows how air comes inside the chimney, which is then extracted from the offices through the chimney opening.

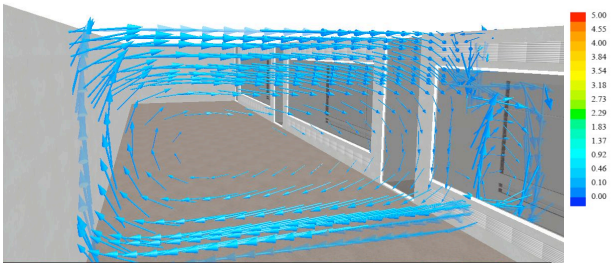

Figure 14. Velocity vectors in the room

Figure 14 shows the section of air-flow path inside the cavity and shafts and how air from the office outlet is directed outside. The air is basically induced to flow upwards by a buoyancy effect created by the accumulated heat. Figure 15 illustrates how the flow reaches higher velocities within the inlet and outlet where pressures are higher. As depicted, flow tends to be turbulent near the glazed surfaces and openings where forces are higher. The airflow inside the cavity is much higher than what is measured by typical examples in the literature.

The airflow inside the room is illustrated in figure 15. The figure shows an air-movement trend from laminar close to the wall boundaries to turbulent in the room's center. The airflow inside the rooms is less than 1 m/s and more than 0.1 m/s.

Table 2. The simulation results are illustrated in the table below:

Simulation	Floor Level	Temp C	Air Velocity	Radiant Temp	RH %	PMV	OT
May	3	20	0.28	22.93	40.7	0.18	20.22
	5	22.4	0.16	22.53	47.3	0.29	20.3
	7	24.8	0.11	33.64	45.59	0.37	20.56
June	3	23.7	0.20	27	51.1	0.5	20
	5	24	0.19	37.50	50.68	0.66	21.30
	7	24.6	0.15	27.19	56.60	0.76	21.09
Sep	3	23.4	0.27	26.3	50.3	0.4	24
	5	23.7	0.20	26.25	57.40	0.54	25.38
	7	24.2	0.13	25.98	56.35	0.71	25.20
Oct	3	22	0.27	23.3	36.4	-0.32	22
	5	22.3	0.20	23.4	42.4	0.11	22.80
	7	22.8	0.19	24.6	45.4	0.23	22.04

Table 3. Calculated air velocity in the office room: 0.5 meter from the windows and 1 meter from the floor.

Ke RNG Turbulence Model					
	Run Details			Model Results	
Model	Grid number	Run time	iterations	ΔT cavity inlet and exhaust	Airflow rate($\frac{m^3}{hr}$)
	5,000,000	72 hours	1000	13.2	102.5

FINDINGS AND ANALYSIS

The results for a south-facing, combined shaft-corridor DSF with external wind velocity of 5 m/s and 50 percent air humidity, respectively, are tabulated in Table 2. Results for the combined shaft-corridor DSF type as shown in Figure indicate that the DSF air gap size of 300 mm gives a comfortable result for these particular conditions in a natural ventilated space.

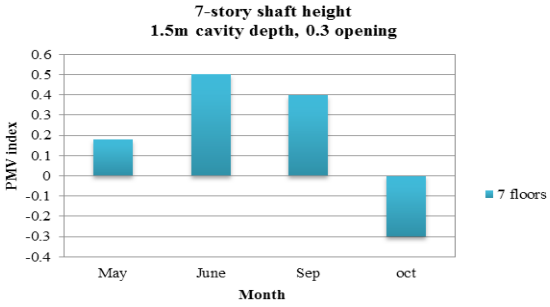

Figure 15. Average PMV index first floor months under study

The office space's lower floors would generate the lowest operative temperature due to the stack effect provided by the DSF configuration. This has enhanced the natural ventilation strategy to provide better internal thermal comfort condition.

There is an internal temperature difference of 1 °C for the DSF mid-floor, which could be due to slower internal air velocity generated. The south-facing DSF configuration produced an 82 percent acceptability limit for the 0.3 m opening for external temperature 23°C, according to the Thermal Environmental Conditions for Human Occupancy from ANSI/ASHRAE Standard 55-2004.

Figure 16 shows the PMV ranges for naturally ventilated spaces with 80 percent acceptable limits indicated for the third floor in May. This graph shows

that there are broader acceptable temperature ranges for naturally ventilated spaces. Air movements determine convective heat and mass exchange of the human body with the surrounding air. In the Chicago climate, high air velocities will increase the evaporation rate at the skin surface, which results in a cooling sensation. The recommended upper limit of indoor air movement is usually 0.8 m/s for human comfort; such air velocity permits the interior space to be 1-2 degrees higher than the human comfort temperature to maintain desirable a comfort level (Hien et al, 2005).

It was found that the combined shaft-corridor DSF will generate a strong stack effect within the air gap, which, in turn, will pull more air out from the office space through rear-wall vents. The temperature generated within the office space is then desirable and close to the human comfort requirement. The airflow pattern created will have a good ventilation effect with cool air coming from the vents, and across and above the internal space, and discharge through the inner pane high level opening.

CONCLUSION

The simulation of the combined shaft-corridor DSF was carried out seven story stack high to investigate the thermal behavior of this new design facade and evaluate the processes involved in thermal comfort. Fluent was used to simulate turbulent airflow. A process was also described to use pre-determined wind pressure values at the cavity's openings to model a DSF cavity in a CFD model. This method reduces computation time that would be needed to analyze wind effects along with buoyancy forces. CFD models were used to determine velocities at various points on the building for wind velocity of 5 m/s based on the weather data. Based on airflow modeling of the combined shaft-corridor DSF, it was found that the stack encourages buoyancy and induces air movement. Convective forces inside the cavity could be used to promote air extraction from the room, although it is needed to promote air movement within the room to release the excess heat.

The CFD results appear to confirm the design's effectiveness in two ways. First, the airflow follows the ceiling and exits through the chimney openings, which suggests that the cool night air will effectively draw the heat out of the ceiling slab. The second outcome of the airflow staying near the ceiling is the avoidance of high air velocities in the occupied zone during the day. This study has shown that the combined shaft-corridor DSF has a possibility of providing acceptable internal thermal comfort through natural ventilation strategy in a hot summer continental climate.

REFERENCES

Afonso, C., and Oliveira, A. (2000). A Solar chimneys: Simulation and experiment. *Energy and Buildings,* 32(1), 71-79.

A.G Davenport. 1963 proceedings of the conference on wind effects on buildings and structures, vol 1. HMSO ,1965

Arons, D. (2000). Properties and Applications of Double-Skin Building Facades. MSc thesis in Building Technology, Massachusetts Institute of Technology (MIT), USA. Web address: http://libraries.mit.edu/docs

Azarbayjani, M. "Energy performance assessment of a naturally ventilated combined shaft-corridor DSF in an office building in Chicago", ARCC 2011, Detroit MI.

Azarbayjani, M. "Integration of natural ventilation in high-rise building with double skin façade", BESS 2011, Pamona, CA.

Champagne, C. (2002). Computational Fluid Dynamics and Double Skin Facades. Assignment for the Architectural Engineering Computer Labs, Pennsylvania State University, USA. Web address: http://www.arche.psu.edu/courses/ae597J/Champage-Hw1.pdf

Gratia, E., and De Herde, A. 2004. "Natural ventilation in a double-skin facade." *Energy and Buildings*, 36(2), 137-146

Hamza, N., and Underwood C, 2005. "CFD supported modeling of double skin facades in hot arid climates", 9th International IBPSA Conference Building Simulation 2005, Vol 1, Montreal (Canada). 365-372.

Hensen, J. 2003. Paper Preparation Guide and Submission Instruction for Building Simulation 2003 Conference, Eindhoven, The Netherlands

Hien, W. N., Liping, W., Chandra, A. N., Pandey, A. R., & Xiaolin, W. (2005). Effects of double glazed facade on energy consumption, thermal comfort and condensation for a typical office building in Singapore. *Energy & Buildings, 37*(6), 563-572.

Macdonald, A. Melikov, Z. Popiolek, P. Stankov (2002), "Integrating CFD and building simulation", Building and Environment 37, pp. 865-871.

Mitchell, J.W., Beckman, W.A. 1995. Instructions for IBPSA Manuscripts, SEL, University of Wisconsin, Madison, WI.

Navvab, M., 2005. "Full scale testing and computer simulation of a double skin façade building." 9th International IBPSA Conference Building Simulation 2005, Vol 2, Montreal (Canada). 831-838.

Oesterle, E., Leib, R.D., Lutz, G., Heusler, B. (2001). Double skin facades: integrated planning: building physics, construction, aerophysics, air-conditioning, economic viability, Prestel, Munich.

Safer, N., Woloszyn M., Roux J.J., Kuznik F.,2005, "Modeling of the double skin facades for building

energy simulation: radiative and convective heat transfers." 9th International IBPSA Conference Building Simulation 2005, Vol 2, Montreal (Canada). 1067-1074.

Stec, W., and Passen D., 2003. " Defining the performance of the double skin façade with the use of the simulation model." 8th International IBPSA Conference Building Simulation 2003, Vol 2, Eindhoven (Netherlands). 1243-1250.

Torres, M., Alavedra P., Guzman A., 2007, "Double skin facades-Cavity and Exterior openings Dimensions for Saving energy on Mediterranean climate." IBPSA Proceedings of Building Simulation 2007, 198-205.

Wong, P.C., Prasad, D., Behnia, M. (2008). A new type of double-skin facade configuration for the hot and humid climate. *Energy and Buildings*, *40*(10), pp. 1941-1945.

Zöllnera, A. Wintera, E. R. F. and Viskanta, R. (2002)"Experimental studies of combined heat transfer "in turbulent mixed convection fluid flows in double-skin-façades." International Journal of Heat and Mass Transfer, 45(22), 4401-4408.